

The Anharmonic Origin of the Giant Thermal Expansion of NaBr

Y. Shen,^{1,*} C. N. Saunders,¹ C. M. Bernal,¹ D. L. Abernathy,² M. E. Manley,³ and B. Fultz^{1,†}

¹*Department of Applied Physics and Materials Science,
California Institute of Technology, Pasadena, California 91125, USA*

²*Neutron Scattering Division, Oak Ridge National Laboratory, Oak Ridge, Tennessee 37831, USA*

³*Materials Science and Technology Division, Oak Ridge National Laboratory, Oak Ridge, Tennessee 37831, USA*

(Dated: September 10, 2019)

All phonons in a single crystal of NaBr were measured by inelastic neutron scattering at temperatures of 10, 300 and 700 K. Even at 300 K the phonons, especially the longitudinal-optical (LO) phonons, showed large shifts in frequencies, and showed large broadenings in energy owing to anharmonicity. *Ab initio* computations were first performed with the quasiharmonic approximation (QHA), in which the phonon frequencies depend only on V , and on T only insofar as it alters V by thermal expansion. This QHA was an unqualified failure for predicting the temperature dependence of phonon frequencies, even 300 K, and the thermal expansion was in error by a factor of four. *Ab initio* computations that included both anharmonicity and quasiharmonicity successfully predicted both the temperature dependence of phonons and the large thermal expansion of NaBr. The frequencies of LO phonon modes decrease significantly with temperature owing to the real part of the phonon self-energy from explicit anharmonicity, originating from the cubic anharmonicity of nearest-neighbor Na-Br bonds. Anharmonicity is not a correction to the QHA predictions of thermal expansion and thermal phonon shifts, but dominates the behavior.

Thermal expansion, a fundamental thermophysical property, originates primarily from a competition between the elastic energy of expansion and the phonon entropy, which usually increases beyond harmonic behavior as a solid expands. Thermal expansion can be calculated readily in the quasiharmonic approximation (QHA), which assumes that phonon frequencies depend only on volume [1–6]. The QHA theory of thermal expansion is textbook content and is logically self-consistent. It ignores explicit anharmonicity, where phonon frequencies also change with temperature at a fixed volume [7, 8]. Some calculations include anharmonicity as a small correction to the QHA, but the relative importance of anharmonicity is not yet settled [2, 9].

We recently found that the QHA gave the wrong sign for the temperature dependence of most phonons in silicon [10]. This shows that the QHA is physically incomplete, even though it did predict correctly the thermal expansion. Here we report a more compelling inelastic neutron scattering (INS) experiment to test predictions of phonons and thermal expansion in a different material, sodium bromide (NaBr). Like other alkali halides with the rocksalt structure [11–13], NaBr has received special attention owing to its cubic structure and highly ionic bonding.

The INS data from a single crystal of NaBr were acquired with the time-of-flight spectrometer, ARCS [14], at the Spallation Neutron Source at the Oak Ridge National Laboratory, using neutrons with an incident energy of 30 meV. Data were collected from 201 rotations of the crystal in increments of 0.5° about the vertical [001] axis. Data reduction gave the 4D scattering func-

tion $S(\mathbf{Q}, \varepsilon)$ [15, 16], where \mathbf{Q} is the 3D wave-vector and ε is the phonon energy (from the neutron energy loss). Nonlinearities of the ARCS instrument were corrected with a small linear rescaling of the q -grid, calibrated by the positions of 45 *in situ* Bragg diffractions. After subtracting the background from measurements on an empty can at the same temperature, and removing multiphonon scattering with the incoherent approximation, the higher Brillouin zones were folded back into an irreducible wedge in the first Brillouin zone to obtain the spectral intensities shown in Fig. 1. The *Supplemental Material* [17] describes the experiment and data analysis in more detail.

The QHA uses an explicit dependence of phonon frequencies on volume into the Helmholtz free energy

$$F^{\text{QHA}}(T, V) = U_0(V) + \sum_{\mathbf{q},j} \left[\frac{\hbar\omega_{\mathbf{q},j}}{2} + k_B T \ln \left(1 - e^{-\frac{\hbar\omega_{\mathbf{q},j}}{k_B T}} \right) \right], \quad (1)$$

where $U_0(V)$ is the ground-state internal energy without any vibrational contribution and the term $k_B \ln[\dots]$ includes the entropy that depends on volume through the individual phonon frequencies $\omega_{\mathbf{q},j} = \omega_{\mathbf{q},j}(V)$ (for the j -th phonon branch at wavevector \mathbf{q}). The finite-displacement method, as implemented in PHONOPY [18], was used to obtain phonon frequencies for different volumes by density functional theory (DFT) calculations with the VASP package [19–22]. The equilibrium volume at a given temperature T was obtained by minimizing $F^{\text{QHA}}(T, V)$ with respect to volume V , keeping T as a fixed parameter. Figure 2 shows how the QHA fails to predict both the magnitude and shape of the thermal expansion curve of NaBr, even at room temperature.

Anharmonic behavior was calculated by the stochastically-initialized temperature dependent effective potential method (sTDEP) [23–26]. In sTDEP,

* yshen@caltech.edu

† btf@caltech.edu

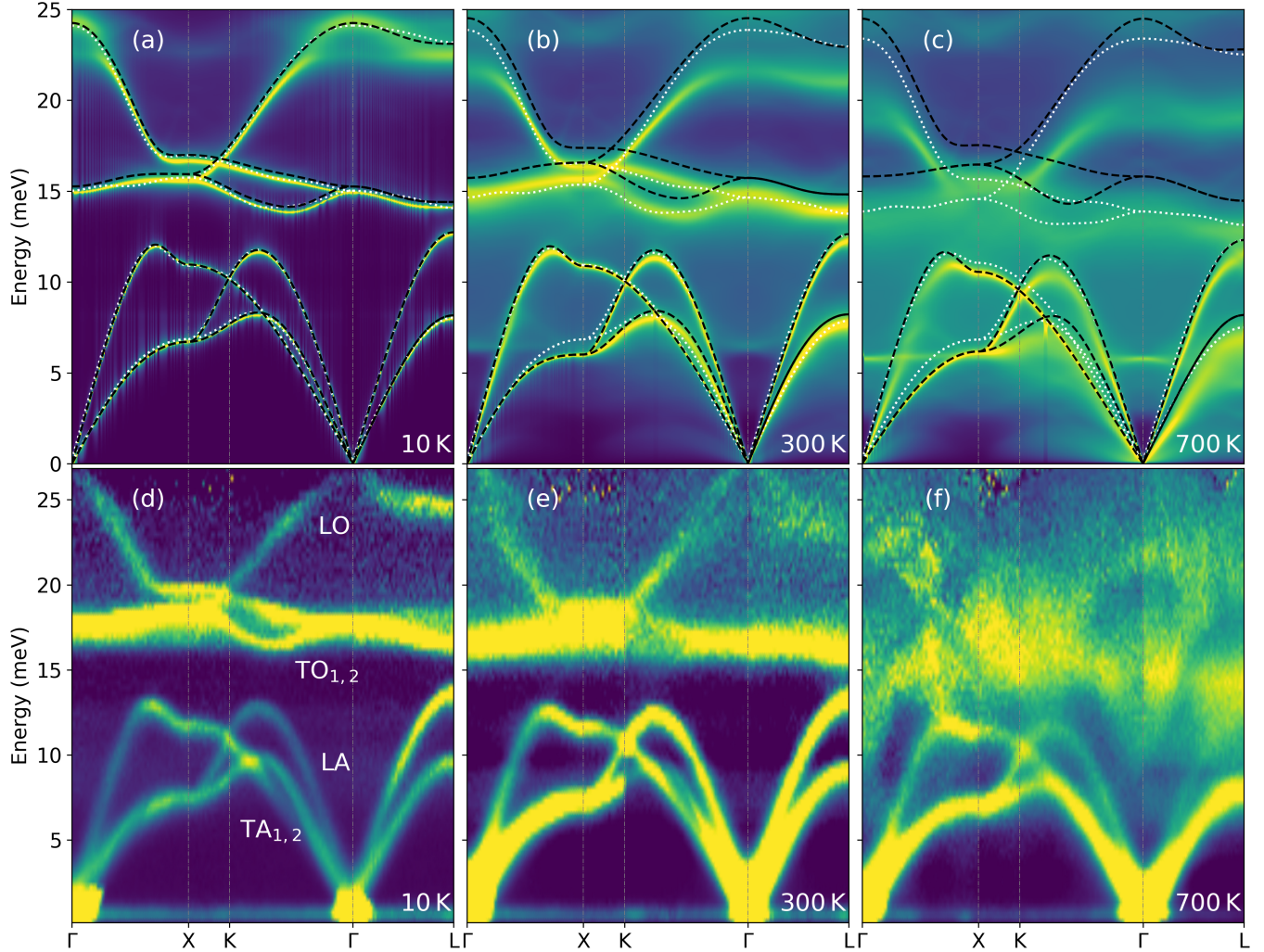


FIG. 1. Comparison between computational (QHA and fully anharmonic) and experimental (INS) results on phonon dispersions of NaBr. (a-c) Phonons in NaBr calculated with the QHA (white dotted line), with only the second-order force constants from sTDEP (black dashed line), and from the full phonon spectral function (logarithmic intensity map) from sTDEP. Temperatures are labeled in the panels. (d-f) Corresponding 2D slices through the four-dimensional scattering function $S(\mathbf{Q}, \varepsilon)$, where $\varepsilon = \hbar\omega$, along high symmetry lines in the first Brillouin zone.

the Born-Oppenheimer molecular dynamics potential energy surface of NaBr was evaluated by a Monte Carlo sampling of the phase space of atom positions. The forces on atoms were fitted to a model Hamiltonian

$$\hat{H} = U_0 + \sum_i \frac{\mathbf{p}_i^2}{2m_i} + \frac{1}{2!} \sum_{ij} \sum_{\alpha\beta} \Phi_{ij}^{\alpha\beta} u_i^\alpha u_j^\beta + \frac{1}{3!} \sum_{ijk} \sum_{\alpha\beta\gamma} \Phi_{ijk}^{\alpha\beta\gamma} u_i^\alpha u_j^\beta u_k^\gamma, \quad (2)$$

by DFT calculations on various configurations of displaced atoms by stochastic sampling of a canonical ensemble, with Cartesian displacements (u_i^α) normally distributed around the mean thermal displacement. The U_0 is a fit parameter for the baseline of the potential energy surface. The quadratic constants Φ_{ij} capture not only

harmonic properties, but their temperature dependence accounts for quartic and higher nonharmonic parts of the potential. These temperature-dependent $\{\Phi_{ij}\}$ were used to calculate phonon frequencies. The cubic force constants Φ_{ijk} capture the broadening and additional shifts of phonon modes, discussed below.

For a given temperature, the Helmholtz free energy $F(T, V)$ was calculated for different volumes V as [27]

$$F(T, V) = U_0(T, V) + F_{\text{vib}}(T, V), \quad (3)$$

where $U_0(T, V)$ is the baseline from Eq. 2. The equilibrium volumes were obtained by minimization of the Helmholtz free energy at T , giving the results shown in Fig. 2. These equilibrium volumes are in good agreement with experimental measurements, although there are deviations at higher temperatures. Details of the cal-

culations of equilibrium volumes and phonon dispersions are given in the *Supplemental Material* [17].

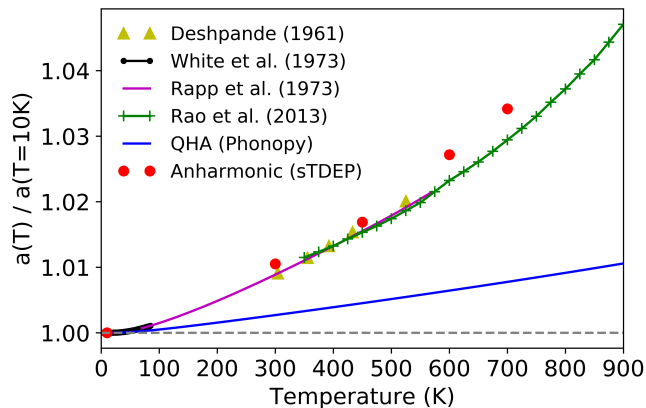


FIG. 2. Thermal expansion of NaBr. The *ab initio* QHA (blue solid line) and anharmonic calculations (red solid circles) are compared with experimental results [28–31]. There is a large discrepancy between the measurements and the QHA predictions, while results from the sTDEP method are in close agreement with the experiments.

Some calculated phonon spectral weights are compared to experimental measurements in Fig. 1 along directions of high symmetry. At 10 K, all calculations agree with each other and with the experimental measurements. At higher temperatures, the acoustic dispersions below 14 meV show some softening, especially at 700 K, but are not broadened so much as the optical modes. The optical modes show large broadening at 300 K, and major changes in shape at 700 K. The temperature dependence of the optical dispersions is largely captured by the spectral weight calculated by sTDEP, but only a minor part of the softening is predicted by the QHA calculations (and none of the broadening owing to its assumption of non-interacting modes). The quadratic term from sTDEP (with $\Phi_{ij}^{\alpha\beta}$ in Eq. 2) was used to calculate the dispersions shown as black dashed lines in Fig. 1a-c. By itself, this term does not reproduce the thermal phonon softening. The largest contribution to the temperature shift of the spectral weight is from the real part of the cubic term, obtained as a Kramers–Kronig transformation of the imaginary part of the self-energy as explained in the *Supplemental Material* [17] with Eq. 51. The imaginary part of the phonon self-energy from this cubic term is responsible for the surprisingly-large energy broadening of the longitudinal optical (LO) phonons at 300 K and especially at 700 K.

The experimental inelastic neutron scattering (INS) measurements (see Fig. 1) were fitted to give the energy shifts of LO phonons presented in Table I. The QHA accounts for only a small part of the experimental shifts, but the anharmonic calculations are much more successful. The spectral intensities at the L -point are shown in Fig. 3a. All phonons at the L -point soften and broaden significantly with temperature. Spectra from the longi-

tudinal acoustic (LA) and transverse optic (TO) phonon modes merge into one broad peak at 700 K. The longitudinal optical (LO) peak broadens significantly, but its large thermal softening is still evident. Figure 3b shows that the real part of the self-energy of the LO phonon at the L -point is approximately -3.5 meV at 700 K, so phonon-phonon anharmonicity dominates the thermal shift of this mode (the LO mode has a phonon energy of 19 meV at the L -point from sTDEP). The *Supplemental Material* [17] shows some of the spectral weights in more detail. There are differences between experiment and the sTDEP calculations at 700 K, especially halfway between Γ and L between 16 and 23 meV. Some anharmonic effects in NaBr are too large to be predicted accurately by the sTDEP method.

To understand the origin of the anharmonicity at 700 K, the cubic irreducible force constants (IFCs) for the three-body interactions within the first ten coordination shells were individually set to zero while recalculating phonon lineshapes at different \mathbf{Q} . Figure 3c shows how two related IFCs dominate the lineshapes. They correspond to the nearest-neighbor cubic interactions of degenerate triplets (NaNaBr and/or NaBrBr) in the [100] direction (i.e. along the Na-Br bond direction). (By translational invariance, $\Phi_{\text{NaNaBr}}^{\alpha\alpha\alpha} = -\Phi_{\text{NaBrBr}}^{\alpha\alpha\alpha}$.) When these force constants are switched off, the phonon lineshapes revert to narrow Lorentzian functions typical of weakly anharmonic solids, and these Lorentzian peaks are at energies similar to those from the QHA calculations. The dominance of $\Phi_{\text{NaNaBr}}^{\alpha\alpha\alpha} = -\Phi_{\text{NaBrBr}}^{\alpha\alpha\alpha}$ on the phonon anharmonicity was found for phonons at all other points in reciprocal space, as shown in the *Supplemental Material* [17].

The physics of thermal expansion requires volume and temperature derivatives of $F(V, T)$, specifically $\partial^2 F / (\partial V \partial T) = -\beta B_T$. The *Supplemental Material* [17] obtains an expression for the ratio between β^{QH} , the thermal expansion in the QHA, and the real β . For $\hbar\omega_{\text{max}} < k_B T$,

$$\beta^{\text{QH}} / \beta = 1 - \frac{6k_B}{\beta B_T v} \bar{\gamma}_{v,T}, \quad (4)$$

where B_T is the isothermal bulk modulus, v is the volume per atom, the mode anharmonicity parameter is

$$\bar{\gamma}_{v,T} \triangleq -\frac{VT}{\omega} \left(\frac{\partial^2 \omega}{\partial T \partial V} \right), \quad (5)$$

and $\bar{\gamma}_{v,T}$ is the average anharmonicity parameter. For NaBr, $\beta^{\text{QH}} \simeq 0.28\beta$, which is consistent with Fig. 2 above.

By testing different first-principles calculations against phonons measured by inelastic neutron scattering at different temperatures, we demonstrated that the widely-accepted quasiharmonic method predicts only a small fraction of the thermal phonon shifts and the thermal expansion. Anharmonic effects drastically alter the phonon self energies, especially the LO phonons. The dominant

TABLE I. Phonon energy shifts of the LO mode with temperature.

T (K)	Energy shift: $(\varepsilon - \varepsilon_{10\text{K}})/\varepsilon_{10\text{K}}$								
	At L -point			Along Γ - L			Along Γ - X		
	QH	Anh.	Exp.	QH	Anh.	Exp.	QH	Anh.	Exp.
300	-0.003	-0.065	-0.080 (0.020)	-0.037	-0.087	-0.062 (0.020)	-0.031	-0.051	-0.052 (0.020)
700	-0.025	-0.164	-0.174 (0.055)	-0.045	-0.181	-0.169 (0.055)	-0.034	-0.144	-0.132 (0.055)

QH = quasiharmonic, Anh. = anharmonic, Exp. = experimental.

Errors are from the instrument energy resolution and/or the peak fitting process.

Average values were used for evaluation along the path.

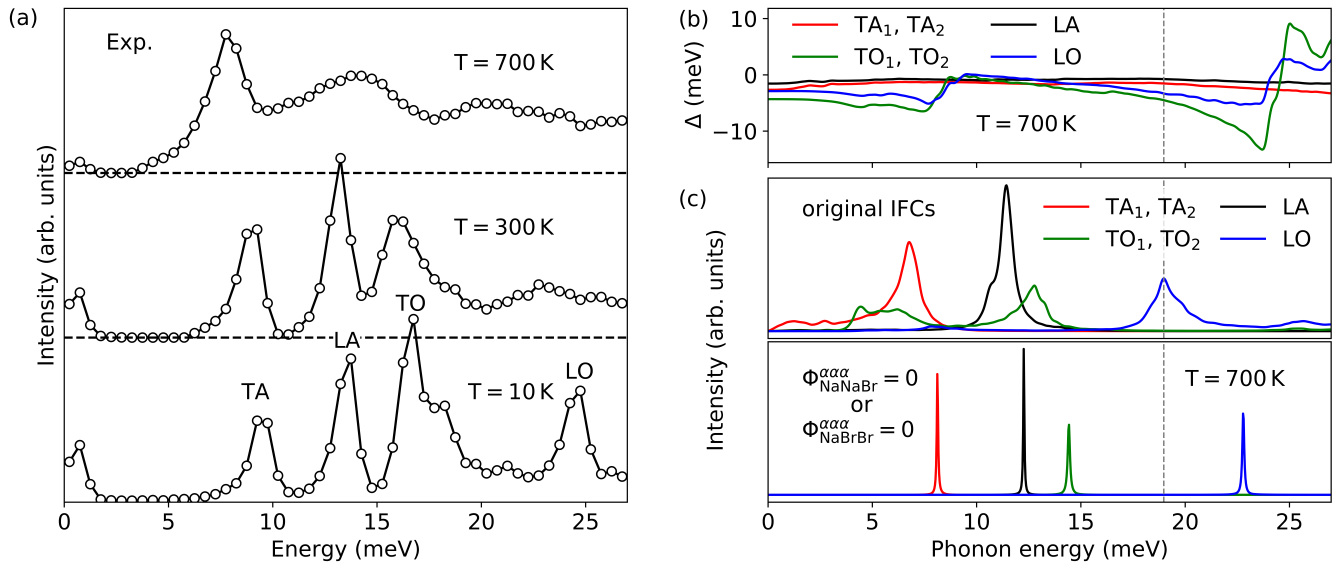


FIG. 3. Measured and calculated phonon lineshapes at the L -point and the real part of the phonon self-energy. (a) The 1D cut of $S(\mathbf{Q}, \varepsilon)$ at a constant $\mathbf{Q} = [0.5, 0.5, 0.5]$ r.l.u. (reciprocal lattice units), showing the temperature dependence of phonon lineshapes. (The small peak near zero is the residue from elastic scattering after correcting for the phonon creation thermal factor.) (b) Real component of the phonon self-energy Δ from the third-order force constants. (c) Phonon intensities after nulling the third-order force constants, $\Phi_{\text{NaNaBr}}^{\alpha\alpha\alpha}$ or $\Phi_{\text{NaBrBr}}^{\alpha\alpha\alpha}$, associated with the nearest-neighbor degenerate triplets, where $\alpha = (x, y, z)$ represents the direction along the Na-Br bond.

anharmonicity is from cubic interactions associated with the nearest-neighbor degenerate triplets along the Na-Br bonding direction. The volume dependence of the phonon anharmonicity dominates the thermal expansion of NaBr, and may do so in many other materials.

We thank D. Kim, O. Hellman, F. Yang and J. Lin for helpful discussions. Research with the Spallation Neutron Source (SNS) at the Oak Ridge National Labora-

tory was sponsored by the Scientific User Facilities Division, Basic Energy Sciences (BES), Department of Energy (DOE). This work used resources from National Energy Research Scientific Computing Center (NERSC), a DOE Office of Science User Facility supported by the Office of Science of the US Department of Energy under Contract DE-AC02-05CH11231. This work was supported by the DOE Office of Science, BES, under Contract DE-FG02-03ER46055.

[1] Z.-K. Liu, Y. Wang, and S. Shang, *Sci. Rep.* **4**, 7043 (2014).
 [2] P. B. Allen, *arXiv preprint arXiv:1906.07103* (2019).
 [3] R. Mittal, M. Gupta, and S. Chaplot, *Prog. Mater. Sci.* **92**, 360 (2018).
 [4] P. Nath, J. J. Plata, D. Usanmaz, R. A. R. A. Orabi, M. Fornari, M. B. Nardelli, C. Toher, and S. Curtarolo, *Comput. Mater. Sci.* **125**, 82 (2016).
 [5] G. Grimvall, *Thermophysical properties of materials* (Elsevier, North-Holland, 1999).

[6] A. Quong and A. Liu, *Phys. Rev. B* **56**, 7767 (1997).
 [7] K. Zakharchenko, M. Katsnelson, and A. Fasolino, *Phys. Rev. Lett.* **102**, 046808 (2009).
 [8] C. W. Li, X. Tang, J. A. Muñoz, J. B. Keith, S. J. Tracy, D. L. Abernathy, and B. Fultz, *Phys. Rev. Lett.* **107**, 195504 (2011).
 [9] A. Erba, M. Shahrokhi, R. Moradian, and R. Dovesi, *J. Chem. Phys.* **142**, 044114 (2015).

- [10] D. S. Kim, O. Hellman, J. Herriman, H. L. Smith, J. Y. Y. Lin, N. Shulumba, J. L. Niedziela, C. W. Li, D. L. Abernathy, and B. Fultz, *Proc. Natl. Acad. Sci. U.S.A.* **115**, 1992 (2018).
- [11] V. Mitskevich, *Sov. Phys. Solid State* **3**, 2202 (1962).
- [12] E. Cowley and R. A. Cowley, *P. Roy. Soc.* **287**, 259 (1965).
- [13] R. Cowley, *Rep. Prog. Phys.* **31**, 123 (1968).
- [14] D. L. Abernathy, M. B. Stone, M. Loguillo, M. Lucas, O. Delaire, X. Tang, J. Lin, and B. Fultz, *Rev. Sci. Instrum.* **83**, 015114 (2012).
- [15] R. Ewings, A. Buts, M. Le, J. van Duijn, I. Bustinduy, and T. Perring, *Nucl. Instrum. Methods Phys. Res. A* **834**, 132 (2016).
- [16] C. W. Li, O. Hellman, J. Ma, A. F. May, H. B. Cao, X. Chen, A. D. Christianson, G. Ehlers, D. J. Singh, B. C. Sales, and O. Delaire, *Phys. Rev. Lett.* **112**, 175501 (2014).
- [17] See Supplemental Material at [URL will be inserted by publisher] for a detailed description of the calculations and experiments.
- [18] A. Togo and I. Tanaka, *Scr. Mater.* **108**, 1 (2015).
- [19] G. Kresse and J. Hafner, *Phys. Rev. B* **47**, 558 (1993).
- [20] G. Kresse and J. Hafner, *Phys. Rev. B* **49**, 14251 (1994).
- [21] G. Kresse and J. Furthmüller, *Comput. Mater. Sci.* **6**, 15 (1996).
- [22] G. Kresse and J. Furthmüller, *Phys. Rev. B* **54**, 11169 (1996).
- [23] O. Hellman, I. A. Abrikosov, and S. I. Simak, *Phys. Rev. B* **84**, 180301 (2011).
- [24] O. Hellman, P. Steneteg, I. A. Abrikosov, and S. I. Simak, *Phys. Rev. B* **87**, 104111 (2013).
- [25] O. Hellman and I. A. Abrikosov, *Phys. Rev. B* **88**, 144301 (2013).
- [26] V. Popescu and A. Zunger, *Phys. Rev. B* **85**, 085201 (2012).
- [27] I. Errea, M. Calandra, and F. Mauri, *Phys. Rev. B* **89**, 064302 (2014).
- [28] V. Deshpande, *Acta Cryst.* **14**, 794 (1961).
- [29] G. K. White, J. G. Collins, and K. A. G. Mendelssohn, *Proc. R. Soc. Lond. A* **333**, 237 (1973).
- [30] J. E. Rapp and H. D. Merchant, *J. Appl. Phys.* **44**, 3919 (1973).
- [31] A. S. M. Rao, K. Narender, K. G. K. Rao, and N. G. Krishna, *J. Mod. Phys.* **4**, 208 (2013).

**Supplementary Material for:
The Anharmonic Origin of the Giant Thermal Expansion of NaBr**

Y. Shen,^{1,*} C. N. Saunders,¹ C. M. Bernal,¹ D. L. Abernathy,² M. E. Manley,³ and B. Fultz^{1,†}

¹*Department of Applied Physics and Materials Science,*

California Institute of Technology, Pasadena, California 91125, USA

²*Neutron Scattering Division, Oak Ridge National Laboratory, Oak Ridge, Tennessee 37831, USA*

³*Material Science and Technology Division, Oak Ridge National Laboratory, Oak Ridge, Tennessee 37831, USA*

(Dated: September 10, 2019)

arXiv:1909.03150v1 [cond-mat.mtrl-sci] 6 Sep 2019

* yshen@caltech.edu

† btf@caltech.edu

I. COMPARING THE THERMAL EXPANSION IN QUASIHARMONIC AND ANHARMONIC THEORIES

A. Classical Thermodynamics

The (volumetric) thermal expansion coefficient, β , is defined as

$$\beta = \frac{1}{V} \frac{dV}{dT} \quad (1)$$

at $P = 0$, or at a constant pressure. This Section I obtains β from the thermodynamic free energy $F(V, T)$, which includes the variables of Eq. 1. A good starting point is classical thermodynamics, which provides relationships involving partial derivatives of F with respect to V and T . Thermal expansion requires both types of partial derivatives to second order. Expansion is a change in volume, of course, but thermal expansion occurs with a change of temperature.

We start with a thermodynamic identity

$$\beta = -\frac{1}{B_T} \frac{\partial^2 F}{\partial T \partial V}, \quad (2)$$

where B_T is the isothermal bulk modulus, defined as

$$B_T = -V \frac{\partial P}{\partial V} = V \frac{\partial^2 F}{\partial V^2}. \quad (3)$$

Thus, we have

$$\beta = -\frac{1}{V} \left(\frac{\partial^2 F}{\partial T \partial V} \right) / \left(\frac{\partial^2 F}{\partial V^2} \right). \quad (4)$$

One strategy to calculate thermal expansion is to solve for $f(T, V) \triangleq \frac{\partial F}{\partial V} = 0$ for $V = V(T)$ in quasiharmonic or anharmonic models, and then obtain the thermal expansion coefficient from Eq. 1. This is done for the quasiharmonic approximation in Sect. III with Fig. 2. Here we employ an alternative strategy of calculating Eq. 4 directly. The two approaches are equivalent because

$$\frac{dV}{dT} = -\left(\frac{\partial f}{\partial T} \right) / \left(\frac{\partial f}{\partial V} \right) = -\left(\frac{\partial^2 F}{\partial T \partial V} \right) / \left(\frac{\partial^2 F}{\partial V^2} \right). \quad (5)$$

B. Phonon Statistical Mechanics

We address the underlying physics by calculating the phonon free energy, ignoring possible contributions from electronic or magnetic excitations. The key quantities are the energies $\{\hbar\omega_i\}$, where ω_i is the frequency of a phonon added to the i th vibrational mode. In general, this frequency depends on V and T , $\omega_i(V, T)$. In the ‘‘quasiharmonic approximation’’ (QHA), the ω_i and the phonon free energy depend only on V . In the QHA, the effects of temperature are only from the occupancies of phonon modes. The QHA is convenient for calculating thermal expansion, requiring only a set of mode Grüneisen parameters. It was recently proved that the QHA gives the leading term of the quantity $\partial F / \partial V$ [1], also [2]. This does not guarantee that the QHA gives the leading term of the thermal expansion coefficient, however, because a temperature derivative is still needed. (For example, consider the functional $y = y_0 + \Delta y$, where $y_0 = 100 + 0.001 \sin x$ and $\Delta y = \sin x$. Here the x -derivative is dominated by the small term Δy , rather than the leading term y_0 .)

Less well known are anharmonic theories of thermal expansion developed with many-body theory [3, 4]. To our knowledge, there has been no direct comparison of thermal expansion from the QHA and anharmonic theory, so the goal of this section is an comparison of the relative importance of each.

Ignoring the entropy from free electrons or magnetic excitations, for a simple solid with N atoms the Helmholtz free energy originates with the electronic energy, i.e., the internal energy of the lattice, U_0 , plus the free energy from phonons

$$F = U_0 + F_{\text{ph}}, \quad (6)$$

$$F = U_0 + \left\langle \sum_{\mathbf{k}, j} \left[\frac{1}{2} \hbar \omega_{\mathbf{k}, j} + k_B T \ln \left(1 - e^{-\frac{\hbar \omega_{\mathbf{k}, j}}{k_B T}} \right) \right] \right\rangle_{\text{BZ}}.$$

where $\hbar\omega_{\mathbf{k},j}$ is the phonon energy at the \mathbf{k} -point for the j th phonon branch. The sum is taken over all phonon branches and \mathbf{k} -points in reciprocal space, and $\langle \dots \rangle_{\text{BZ}}$ is the average over the first Brillouin zone. For clarity in what follows, the subscripts of ω are suppressed.

Because the free energy depends on V and T , we expect $U_0 = U_0(V, T)$ and $\omega = \omega(V, T)$. Derivatives of these quantities are needed for Eq. 4. The volume derivative is essential for expansion

$$\begin{aligned} \frac{\partial F}{\partial V} &= \frac{\partial U_0}{\partial V} + \left\langle \sum \frac{\hbar}{2} \frac{\partial \omega}{\partial V} + \frac{k_B T}{1 - e^{-\frac{\hbar\omega}{k_B T}}} \left(-e^{-\frac{\hbar\omega}{k_B T}} \right) \left(-\frac{\hbar}{k_B T} \right) \frac{\partial \omega}{\partial V} \right\rangle_{\text{BZ}} \\ &= \frac{\partial U_0}{\partial V} + \frac{\hbar}{2} \left\langle \sum \frac{\partial \omega}{\partial V} \coth \left(\frac{\hbar\omega}{2k_B T} \right) \right\rangle_{\text{BZ}} . \end{aligned} \quad (7)$$

From Eq. 7, we can calculate the additional derivatives needed in Eq. 4

$$\frac{\partial^2 F}{\partial T \partial V} = \frac{\partial^2 U_0}{\partial T \partial V} + \frac{\hbar}{2} \left\langle \sum \left[\frac{\partial^2 \omega}{\partial T \partial V} \coth \left(\frac{\hbar\omega}{2k_B T} \right) - \frac{\partial \omega}{\partial V} \operatorname{csch}^2 \left(\frac{\hbar\omega}{2k_B T} \right) \left(\frac{\hbar}{2k_B T} \frac{\partial \omega}{\partial T} - \frac{\hbar\omega}{2k_B T^2} \right) \right] \right\rangle_{\text{BZ}} , \quad (8)$$

and

$$\frac{\partial^2 F}{\partial V^2} = \frac{\partial^2 U_0}{\partial V^2} + \frac{\hbar}{2} \left\langle \sum \left[\frac{\partial^2 \omega}{\partial V^2} \coth \left(\frac{\hbar\omega}{2k_B T} \right) - \frac{\partial \omega}{\partial V} \operatorname{csch}^2 \left(\frac{\hbar\omega}{2k_B T} \right) \left(\frac{\hbar}{2k_B T} \frac{\partial \omega}{\partial V} \right) \right] \right\rangle_{\text{BZ}} . \quad (9)$$

C. Internal Energy

The first terms with U_0 in Eqs. 8 and 9 are familiar from the elastic energy of a solid. They are typically obtained from a Taylor expansion of the internal energy. For cubic crystals near the ground-state equilibrium volume V_0 ,

$$U_0(V, T) = U_0(V_0, T) + \frac{B_0(T)V_0}{2} \left(\frac{V - V_0}{V_0} \right)^2 + \dots , \quad (10)$$

gives

$$\frac{\partial U_0}{\partial V} = B_0(T) \left(\frac{V - V_0}{V_0} \right) , \quad (11)$$

then

$$\frac{\partial^2 U_0}{\partial V^2} = \frac{B_0(T)}{V_0} , \quad (12)$$

and

$$\frac{\partial^2 U_0}{\partial T \partial V} = \frac{dB_0}{dT} \left(\frac{V - V_0}{V_0} \right) , \quad (13)$$

where $B_0 = -V(\partial P/\partial V)_{P=0}$ is the zeroth-order bulk modulus (i.e. $B_0 = B_T$).

D. Phonon Contributions at Medium to High Temperatures

To simplify the second terms in Eqs. 8 and 9, notice that $\coth(x) = \frac{1}{x} + \frac{x}{3} - \frac{x^3}{45} + \dots$ and $\operatorname{csch}(x) = \frac{1}{x} - \frac{x}{6} + \frac{7x^3}{360} + \dots$, so for $\hbar\omega_{\max} < k_B T$,

$$\coth \left(\frac{\hbar\omega}{2k_B T} \right) \simeq \operatorname{csch} \left(\frac{\hbar\omega}{2k_B T} \right) \simeq \frac{2k_B T}{\hbar\omega} . \quad (14)$$

Using Eq. 14 greatly simplifies Eq. 8 and 9, with the restriction to higher temperatures where $\hbar\omega_{\max} < k_B T$,

$$\frac{\partial^2 F}{\partial T \partial V} = \frac{dB_T}{dT} \left(\frac{V - V_0}{V_0} \right) + k_B \left\langle \sum \left(\frac{T}{\omega} \frac{\partial^2 \omega}{\partial T \partial V} - \frac{T}{\omega^2} \frac{\partial \omega}{\partial T} \frac{\partial \omega}{\partial V} + \frac{1}{\omega} \frac{\partial \omega}{\partial V} \right) \right\rangle_{\text{BZ}} , \quad (15)$$

and

$$\begin{aligned}
B_T &= V \frac{\partial^2 F}{\partial V^2} \simeq V \left\{ \frac{B_T}{V_0} + k_B T \left\langle \sum \left[\frac{1}{\omega} \frac{\partial^2 \omega}{\partial V^2} - \frac{1}{\omega^2} \left(\frac{\partial \omega}{\partial V} \right)^2 \right] \right\rangle_{\text{BZ}} \right\} \\
B_T &= \frac{V}{V_0} B_T + k_B T V \left\langle \sum \frac{\partial^2 (\ln \omega)}{\partial V^2} \right\rangle_{\text{BZ}},
\end{aligned} \tag{16}$$

which indicates $\left| k_B T V \left\langle \sum \frac{\partial^2 (\ln \omega)}{\partial V^2} \right\rangle_{\text{BZ}} \right| \ll B_T$, since $V/V_0 \simeq 1$.

E. Quasiharmonic Approximation

In the quasiharmonic approximation, $U_0 = U_0(V, T = 0)$ and $\omega = \omega(V, T = 0)$, so

$$\left(\frac{\partial^2 U_0}{\partial V^2} \right)^{\text{QH}} = \frac{B_T(T=0)}{V_0}, \quad \left(\frac{\partial^2 U_0}{\partial T \partial V} \right)^{\text{QH}} = 0, \quad \left(\frac{\partial \omega}{\partial T} \right)^{\text{QH}} = 0. \tag{17}$$

For $\hbar \omega_{\text{max}} < k_B T$, Eqs. 8 and 9 are simplified

$$\left(\frac{\partial^2 F}{\partial T \partial V} \right)^{\text{QH}} = k_B \left\langle \sum \frac{1}{\omega(V, T=0)} \frac{\partial \omega(V, T=0)}{\partial V} \right\rangle_{\text{BZ}}, \tag{18}$$

and

$$B_T^{\text{QH}} = V \left(\frac{\partial^2 F}{\partial V^2} \right)^{\text{QH}} \simeq \frac{V}{V_0} B_T(T=0) + k_B T V \left\langle \sum \frac{\partial^2 [\ln \omega(V, T=0)]}{\partial V^2} \right\rangle_{\text{BZ}} \simeq B_T(T=0) \simeq B_T, \tag{19}$$

assuming B_T is not strongly dependent on temperature, which is often true in practice.

F. Comparison of Quasiharmonic and Anharmonic Results for Thermal Expansion

The results from Sections [ID](#) and [IE](#) allow a direct comparison of the difference in thermal expansion predicted by anharmonic and quasiharmonic theory. For moderate to high temperatures the difference between β and β^{QH} is

$$\begin{aligned}
\beta - \beta^{\text{QH}} &= \left(-\frac{1}{B_T} \frac{\partial^2 F}{\partial T \partial V} \right) - \left(-\frac{1}{B_T^{\text{QH}}} \frac{\partial^2 F^{\text{QH}}}{\partial T \partial V} \right), \\
&\simeq -\frac{1}{B_T} \frac{\partial^2 (F - F^{\text{QH}})}{\partial T \partial V},
\end{aligned}$$

assuming the bulk modulus does not vary strongly with temperature. Using the derivatives of F from Sections [ID](#) and [IE](#)

$$\begin{aligned}
\beta - \beta^{\text{QH}} &= -\frac{1}{B_T} \frac{dB_T}{dT} \left(\frac{V - V_0}{V_0} \right) - \\
&\quad \frac{k_B}{B_T} \left\langle \sum \left(\frac{T}{\omega} \frac{\partial^2 \omega}{\partial T \partial V} - \frac{T}{\omega^2} \frac{\partial \omega}{\partial T} \frac{\partial \omega}{\partial V} + \frac{1}{\omega(V, T)} \frac{\partial \omega(V, T)}{\partial V} - \frac{1}{\omega(V, T=0)} \frac{\partial \omega(V, T=0)}{\partial V} \right) \right\rangle_{\text{BZ}} \\
&\simeq -\frac{1}{B_T} \frac{dB_T}{dT} \left(\frac{V - V_0}{V_0} \right) - \frac{k_B}{B_T} \left\langle \sum \left[\frac{T}{\omega} \frac{\partial^2 \omega}{\partial T \partial V} - \frac{T}{\omega^2} \frac{\partial \omega}{\partial T} \frac{\partial \omega}{\partial V} + T \frac{\partial}{\partial T} \left(\frac{1}{\omega} \frac{\partial \omega}{\partial V} \right) \right] \right\rangle_{\text{BZ}} \\
&= -\frac{1}{B_T} \frac{dB_T}{dT} \left(\frac{V - V_0}{V_0} \right) - \frac{2k_B}{B_T} \left\langle \sum \left(\frac{T}{\omega} \frac{\partial^2 \omega}{\partial T \partial V} - \frac{T}{\omega^2} \frac{\partial \omega}{\partial T} \frac{\partial \omega}{\partial V} \right) \right\rangle_{\text{BZ}} \\
&= -\frac{1}{B_T} \frac{dB_T}{dT} \left(\frac{V - V_0}{V_0} \right) + \frac{2k_B T}{B_T} \left\langle \sum \left(-\frac{1}{\omega} \frac{\partial^2 \omega}{\partial T \partial V} + \frac{1}{\omega^2} \frac{\partial \omega}{\partial T} \frac{\partial \omega}{\partial V} \right) \right\rangle_{\text{BZ}},
\end{aligned} \tag{20}$$

thus we have

$$\begin{aligned}\beta^{\text{QH}}/\beta &= 1 + \frac{1}{B_T\beta} \frac{dB_T}{dT} \left(\frac{V-V_0}{V_0} \right) - \frac{2k_B T}{B_T\beta} \left\langle \sum \left(-\frac{1}{\omega} \frac{\partial^2 \omega}{\partial T \partial V} + \frac{1}{\omega^2} \frac{\partial \omega}{\partial T} \frac{\partial \omega}{\partial V} \right) \right\rangle_{\text{BZ}} \\ &\simeq 1 - \frac{2k_B T}{B_T\beta} \left\langle \sum \left(-\frac{1}{\omega} \frac{\partial^2 \omega}{\partial T \partial V} + \frac{1}{\omega^2} \frac{\partial \omega}{\partial T} \frac{\partial \omega}{\partial V} \right) \right\rangle_{\text{BZ}},\end{aligned}\quad (21)$$

since $\frac{1}{B_T\beta} \frac{dB_T}{dT} \left(\frac{V-V_0}{V_0} \right) < \frac{1}{B_T\beta} \frac{dB_T}{dT} \beta T = \left(\frac{dB_T}{dT} T \right) / B_T \sim 0.1 \ll 1$ (e.g. in MgO [5]).

G. Simplifying Parameters

Introducing the mode Grüneisen parameter,

$$\gamma_v \triangleq -\frac{V}{\omega} \left(\frac{\partial \omega}{\partial V} \right) \Big|_T, \quad (22)$$

the thermal Grüneisen parameter (unitless),

$$\gamma_T \triangleq -\frac{T}{\omega} \left(\frac{\partial \omega}{\partial T} \right) \Big|_V, \quad (23)$$

and the anharmonicity parameter (unitless),

$$\gamma_{v,T} \triangleq -\frac{VT}{\omega} \left(\frac{\partial^2 \omega}{\partial T \partial V} \right), \quad (24)$$

Eq. 21 can be rewritten as

$$\beta^{\text{QH}}/\beta = 1 - \frac{2k_B}{B_T\beta V} \left\langle \sum (\gamma_{v,T} + \gamma_T \gamma_v) \right\rangle_{\text{BZ}}. \quad (25)$$

To first order, the infinitesimal change of phonon energy can be divided into changes induced by temperature and volume

$$\Delta\omega \simeq \frac{\partial \omega}{\partial T} \Delta T + \frac{\partial \omega}{\partial V} \Delta V \triangleq \Delta\omega^T + \Delta\omega^V, \quad (26)$$

we find (for later use in Eq. 21)

$$\begin{aligned}-\frac{1}{\omega} \frac{\partial^2 \omega}{\partial T \partial V} + \frac{1}{\omega^2} \frac{\partial \omega}{\partial T} \frac{\partial \omega}{\partial V} &\simeq -\frac{1}{\omega} \frac{\Delta\omega^T + \Delta\omega^V}{\Delta T \Delta V} + \frac{1}{\omega^2} \frac{\Delta\omega^T}{\Delta T} \frac{\Delta\omega^V}{\Delta V} \\ &= \frac{1}{\Delta T \Delta V} \left[\left(-\frac{\Delta\omega^T}{\omega} \right) + \left(-\frac{\Delta\omega^V}{\omega} \right) + \left(-\frac{\Delta\omega^T}{\omega} \right) \left(-\frac{\Delta\omega^V}{\omega} \right) \right].\end{aligned}\quad (27)$$

For small positive values of $\left(-\frac{\Delta\omega^T}{\omega} \right)$ and $\left(-\frac{\Delta\omega^V}{\omega} \right)$,

$$\left(-\frac{\Delta\omega^T}{\omega} \right) + \left(-\frac{\Delta\omega^V}{\omega} \right) \gg \left(-\frac{\Delta\omega^T}{\omega} \right) \left(-\frac{\Delta\omega^V}{\omega} \right), \quad (28)$$

which gives

$$\beta^{\text{QH}}/\beta \simeq 1 - \frac{2k_B}{B_T\beta V} \left\langle \sum \gamma_{v,T} \right\rangle_{\text{BZ}} = 1 - \frac{2k_B}{B_T\beta V} (3N) \bar{\gamma}_{v,T} = 1 - \frac{6k_B}{B_T\beta v} \bar{\gamma}_{v,T}, \quad (29)$$

where $v = V/N$ is the volume per atom, and $\bar{\gamma}_{v,T} = \frac{1}{3N} \left\langle \sum_{\mathbf{k}} \sum_{j=1}^{3N} \gamma_{v,T}^{(j)} \right\rangle_{\text{BZ}}$ is the average anharmonicity parameter.

An interesting and compact result from Eq. 29 is

$$\beta \simeq \beta^{\text{QH}} + \frac{6k_B}{B_T v} \bar{\gamma}_{v,T}. \quad (30)$$

This shows that the thermal expansion differs from that of the QHA owing to the mixed second derivative of the phonon energy of Eq. 24. In general, thermal expansion requires the consideration of both the volume and temperature dependence of the free energy.

H. Why is the QHA Unreliable for Thermal Expansion?

Eq. 30 shows why the quasiharmonic model predicts a small thermal expansion coefficient when phonon frequencies have a temperature dependence that varies with volume. Only in the limit of no temperature dependence, which means $\bar{\gamma}_{v,T} = 0$, Eq. 30 reduces to $\beta^{\text{QH}} = \beta$. Here we estimate some magnitudes of these effects.

The change of internal energy is estimated as

$$\Delta U_0 = \frac{1}{2} B_0 V_0 \left(\frac{\Delta V}{V_0} \right)^2 \simeq B_0 V \cdot (0.01)^2 \simeq 10^{0 \sim 1} \text{meV}, \quad (31)$$

which gives

$$B_T V = B_0 V \simeq 10^{4 \sim 5} \text{meV} = 10^{1 \sim 2} \text{eV}. \quad (32)$$

Thus,

$$\frac{6k_B}{B_T \beta V} \simeq \frac{6 \times 8.617 \times 10^{-5} \text{eV} \cdot \text{K}^{-1}}{10^{-5 \sim -4} \text{K}^{-1} \cdot 10^{1 \sim 2} \text{eV}} \sim \mathcal{O}(10^{-2 \sim 0}) \text{ [unitless]}, \quad (33)$$

and in some solids, some modes are possible with $0 < \bar{\gamma}_{v,T} \sim \mathcal{O}(1)$.

Finally, we have

$$\beta^{\text{QH}} / \beta \sim 1 - \mathcal{O}(10^{-2 \sim 0}) \cdot \mathcal{O}(1). \quad (34)$$

Under some circumstances, the thermal expansion coefficient can be several times larger than the quasiharmonic prediction, which means the QHA fails to get the first-order term for thermal expansion. If the QHA accounts for the leading term of thermal expansion, it is either because 1) the solid is not so anharmonic ($\bar{\gamma}_{v,T}$ is small), or 2) there is a cancellation of positive and negative $\bar{\gamma}_{v,T}$ for different phonon modes despite the anharmonicity.

I. Estimate of Thermal Expansion of NaBr

We expect these $\gamma_{v,T}$ to differ for the different phonon modes, but usually all these parameters $\gamma_{v,T}$ are not available for all phonon modes. For NaBr, the energies of acoustic phonons have small changes with temperature compared to the energies of optical phonons. We therefore estimate how the thermal expansion of NaBr deviates from the prediction of the QHA by considering only the optical phonons.

At $T = 700 \text{K}$, the fractional energy shifts of the LO phonons are estimated by averaging the shifts along the Γ - L and Γ - X lines as listed in Table I in the manuscript

$$\left\langle -\frac{\Delta\omega^{(\text{LO})}}{\omega} \right\rangle_{\text{BZ}} \simeq -\frac{1}{2} [(-0.169) + (-0.132)] = 0.15. \quad (35)$$

and the anharmonicity parameter by

$$\gamma_{v,x} = -\frac{VT}{\omega} \left(\frac{\partial^2 \omega}{\partial T \partial V} \right) \simeq -\frac{VT}{\omega} \frac{\Delta\omega}{\Delta T \Delta V} = -\frac{\Delta\omega}{\omega} \frac{T}{\Delta T} \frac{V}{\Delta V} \simeq -\frac{\Delta\omega}{\omega} \frac{V}{\Delta V}. \quad (36)$$

With $\frac{a(T=700 \text{K})}{a(T=10 \text{K})} = 1.03$, we have $\frac{V}{\Delta V} = \frac{1.03^3}{1.03^3 - 1} \simeq 11.78$ and thus $\bar{\gamma}_{v,T}^{(\text{LO})} = 1.767$. Similarly, we obtain

$\left\langle -\frac{\Delta\omega^{(\text{TO}_{1,2})}}{\omega} \right\rangle_{\text{BZ}} \simeq 0.14$ and $\bar{\gamma}_{v,T}^{(\text{TO}_{1,2})} = 1.649$ for the two TO modes. The average anharmonicity parameter of NaBr is approximately

$$\bar{\gamma}_{v,T} = \frac{1}{6} \sum_{i=1}^6 \bar{\gamma}_{v,T}^{(i)} \simeq \frac{1}{6} (\bar{\gamma}_{v,T}^{(\text{LO})} + 2\bar{\gamma}_{v,T}^{(\text{TO})}) = 0.844. \quad (37)$$

We take the value of $\beta = 3\alpha = 3 \times 60.63 \times 10^{-6} \text{K}^{-1} = 182 \times 10^{-6} \text{K}^{-1}$ [6], $B_T = 18.5 \text{GPa}$ [7] and $a = 6.1376 \text{\AA}$ (700 K) [6], which gives the volume per atom as $v = a^3/8 = 2.89 \times 10^{-29} \text{m}^3$. So finally,

$$\beta^{\text{QH}} / \beta = 1 - \frac{6k_B}{B_T \beta v} \bar{\gamma}_{v,T} \simeq 0.28, \quad (38)$$

which is rather good agreement with the deficiency of the QHA shown in Fig. 3.

II. INELASTIC NEUTRON SCATTERING EXPERIMENTS

The INS measurements used a high-purity single crystal of NaBr. Crystal quality was checked by X-ray and neutron diffraction. The INS data were acquired with the time-of-flight Wide Angular-Range Chopper Spectrometer, ARCS, at the Spallation Neutron Source at the Oak Ridge National Laboratory. The neutrons had an incident energy of 30 meV. The single crystal of [001] orientation was suspended in an aluminum holder, which was mounted in a closed-cycle helium refrigerator for the 10 K measurement, and a low-background electrical resistance vacuum furnace for measurements at 300 and 700 K. For each measurement, time-of-flight neutron data was collected from 201 rotations of the crystal in increments of 0.5° about the vertical axis.

Data reduction gave the 4D scattering function $S(\mathbf{Q}, \varepsilon)$, where \mathbf{Q} is the 3D wave-vector and ε is the phonon energy (from the neutron energy loss). Measurements with an empty can were performed to evaluate the background. To correct for nonlinearities of the ARCS instrument, offsets of the q -grid were corrected to first order by fitting a set of 45 *in situ* Bragg diffractions, which were transformed to their theoretical positions in the reciprocal space of the NaBr structure. The linear transformation matrix had only a small deviation (less than 0.02) from the identity matrix, showing that the original data had good quality and the linear correction for q -offsets was adequate. After subtracting the empty-can background and removing multiphonon scattering calculated with the incoherent approximation (discussed below), the intensities from the higher Brillouin zones were folded back into an irreducible wedge in the first Brillouin zone to obtain the spectral intensities shown in Fig. 2 in the main text.

The multiphonon scattering in the incoherent approximation [8] is given by

$$S_{n>1}(\mathbf{Q}, \varepsilon) = \sum_{n=2}^{\infty} \sum_d e^{-2W_d} \frac{(2W_d)^n}{n!} \frac{\sigma_{\text{total},d}}{M_d} A_{n,d}(\varepsilon), \quad (39)$$

where \mathbf{Q} is the reciprocal space vector, ε is the phonon energy, and for atom $d \in (\text{Na}, \text{Br})$, $\sigma_{\text{total},d}$ is the total neutron scattering cross section, M_d is atomic mass, and

$$2W_d = 2W_d(|\mathbf{Q}|) = \frac{\hbar^2 |\mathbf{Q}|^2}{2M_d} \int_0^\infty d\varepsilon \frac{g_d(\varepsilon)}{\varepsilon} \coth\left(\frac{\varepsilon}{2k_B T}\right) \quad (40)$$

is the Debye-Waller factor. The n^{th} -order partial phonon spectra of atoms d and \bar{d} , $A_{n,d}$ and $A_{n,\bar{d}}$, were calculated as

$$A_{1,d}(\varepsilon) = \frac{g_d(\varepsilon)}{\varepsilon} \frac{1}{e^{\varepsilon/k_B T} - 1}, \quad (41)$$

$$A_{1,\bar{d}}(\varepsilon) = \frac{g_{\bar{d}}(\varepsilon)}{\varepsilon} \frac{1}{e^{\varepsilon/k_B T} - 1}, \quad (42)$$

$$A_{n,d}(\varepsilon) = \frac{1}{2} \left(A_{1,d} \otimes A_{n-1,d} + \frac{1}{n} A_{1,d} \otimes A_{n-1,\bar{d}} + \frac{n-1}{n} A_{1,\bar{d}} \otimes A_{n-1,d} \right), \quad (43)$$

$$A_{n,\bar{d}}(\varepsilon) = \frac{1}{2} \left(A_{1,\bar{d}} \otimes A_{n-1,\bar{d}} + \frac{1}{n} A_{1,\bar{d}} \otimes A_{n-1,d} + \frac{n-1}{n} A_{1,d} \otimes A_{n-1,\bar{d}} \right). \quad (44)$$

Here, \bar{d} refers to the other atom in the unit cell. The temperature-dependent partial phonon density of states (DOS), $g_d(\varepsilon)$, was obtained by our sTDEP method that used *ab initio* DFT calculations.

For NaBr, we truncated Eq. 39 at $n = 8$, and a global scaling factor was applied to the multiphonon scattering function for normalization. Finally, the folded-back data was corrected for the phonon creation thermal factor. This folding technique cancels out the polarization effects and improves the statistical quality by assessing phonon intensities over multiple Brillouin zones. Fig. 1 shows a set of enlarged, separated figures of the scattering data along the Γ - X and Γ - L directions.

III. AB INITIO CALCULATIONS

A. General

All DFT calculations were performed with the VASP package using a plane-wave basis set [9–12] with projector augmented wave (PAW) pseudopotentials [13] and the Perdew-Burke-Ernzerhof (PBE) exchange correlation functional [14]. All calculations used a kinetic-energy cutoff of 550 meV, a $5 \times 5 \times 5$ supercell of 250 atoms, and a $3 \times 3 \times 3$ k -point grid. Quasiharmonic calculations used PHONOPY [15]. The sTDEP [16–18] method was used to calculate anharmonic phonons at elevated temperatures. The Born effective charges and dielectric constants were obtained by DFT calculations in VASP [19]. The non-analytical term of the long-ranged electrostatics was corrected for both quasiharmonic and anharmonic calculations [20]. The phonon self-energy was calculated with a $35 \times 35 \times 35$ q -grid.

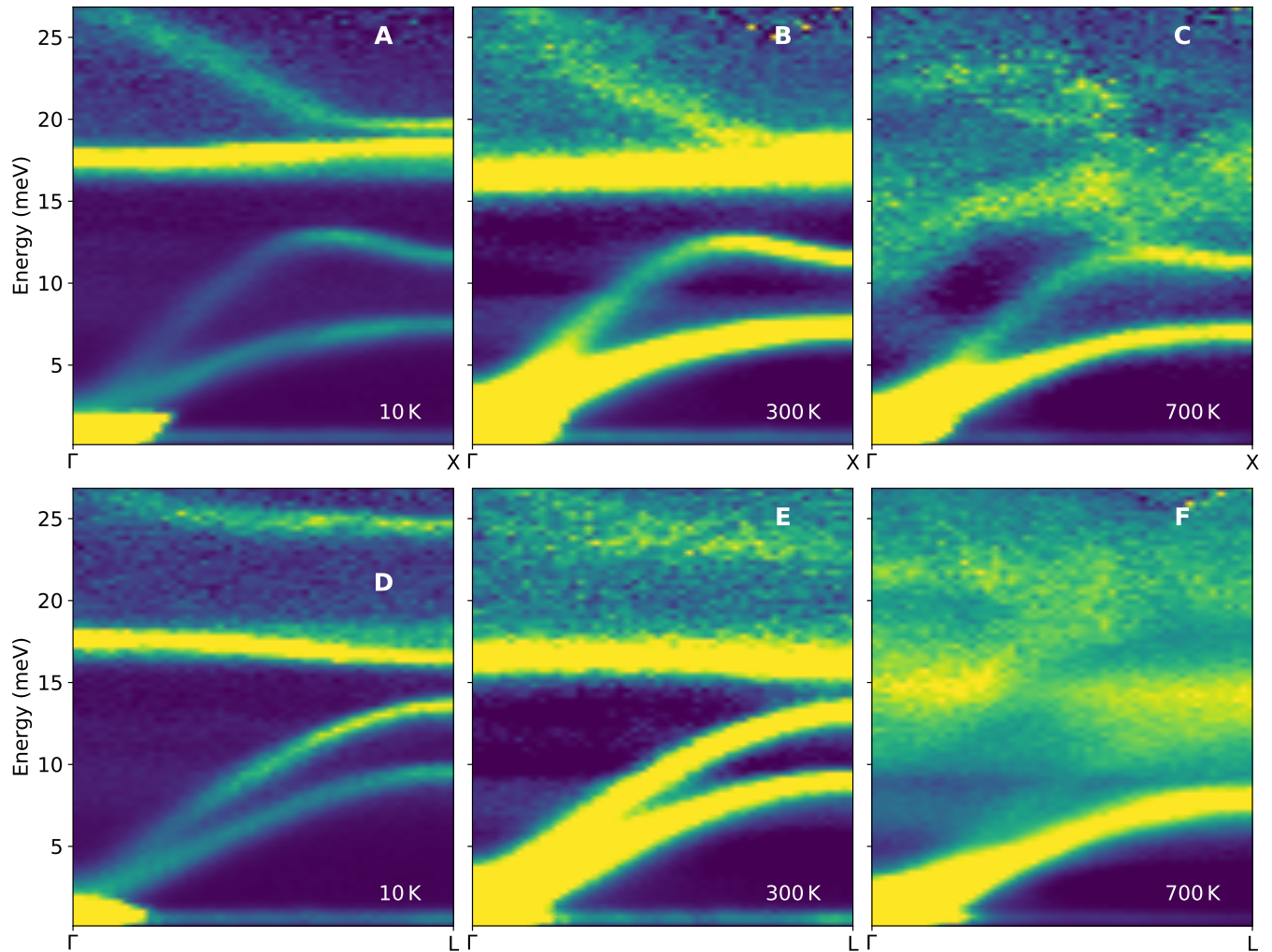


FIG. 1. **Experimental phonon dispersions of NaBr along Γ -X and Γ -L.** Phonon dispersions are shown by 2D slices of the $S(\mathbf{Q}, \varepsilon)$ data along the high symmetry lines of Γ -X (a-c) and Γ -L (d-f) at the temperature of 10 K (a, d), 300 K (b, e) and 700 K (c, f).

B. Quasiharmonic calculations

The free energy and the equilibrium volumes calculated with the QHA are shown in Fig. 2. The linear thermal expansion coefficients from measurements and QHA calculations are compared in Fig. 3. We did not calculate detailed linear thermal expansion coefficients with the stochastically-initialized temperature dependent effective potential method (sTDEP) method, but we compared lattice constants at several temperatures to illustrate thermal expansion (see Fig. 1 in the main text).

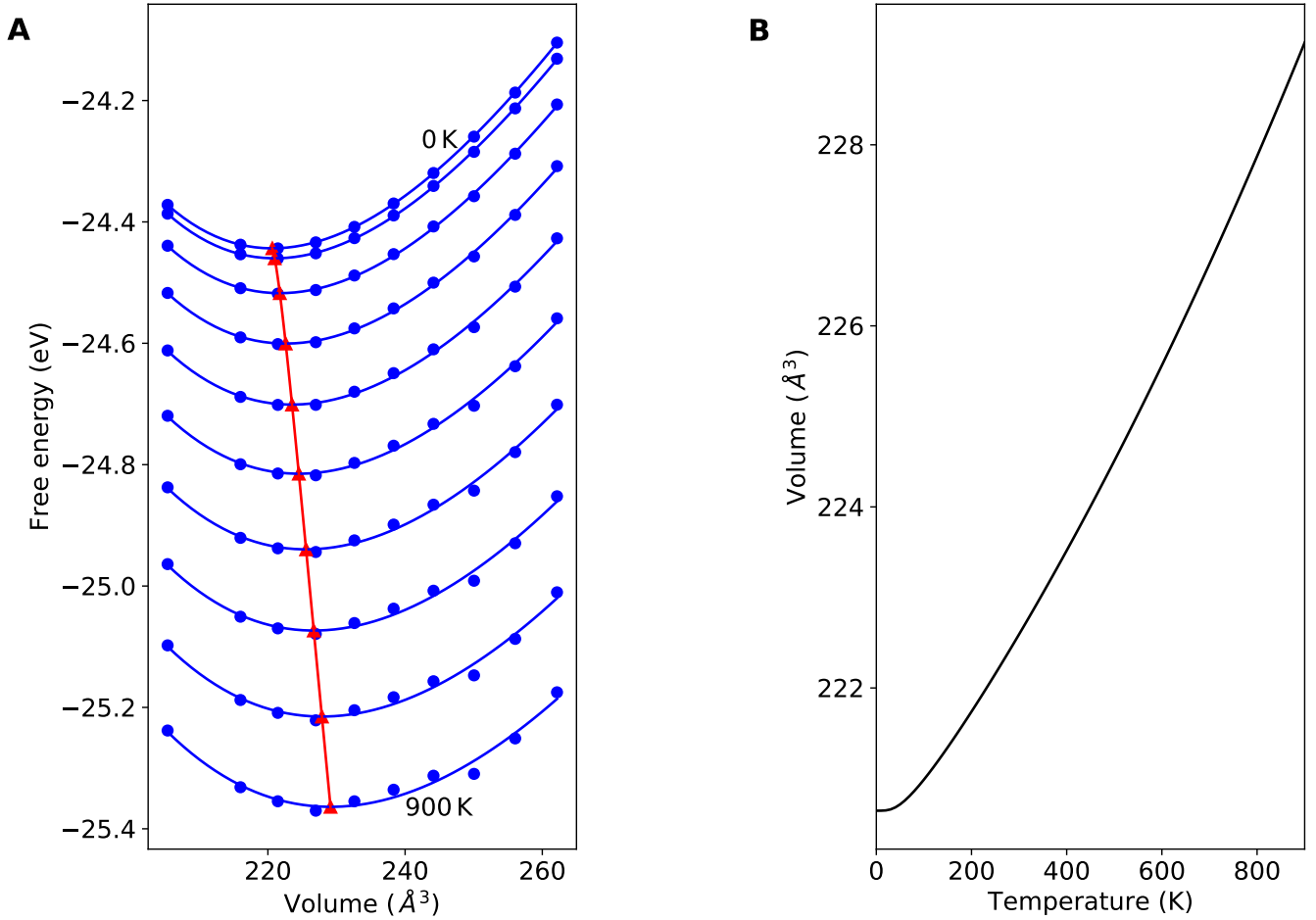


FIG. 2. Intermediate results for expansion coefficients of NaBr calculated with the QHA. **a**, The Helmholtz free energy as a function of temperature and volume. The volume-energy data was fitted to a Birch-Murnaghan equation of state. **b**, The equilibrium volumes with temperature, obtained by minimizing the free energy at each temperature.

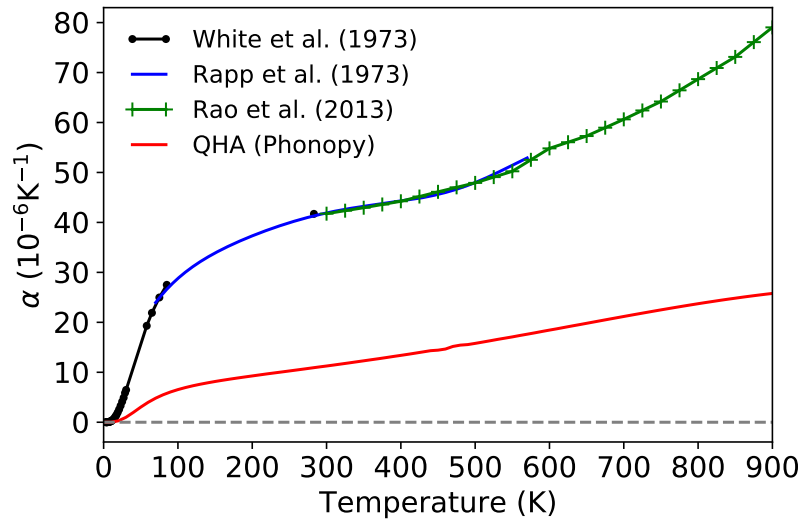


FIG. 3. Thermal expansion coefficients of NaBr, measured and calculated by QHA. The *ab initio* quasiharmonic predictions (red solid line) are compared to the experimental results [6, 21, 22]. The linear thermal expansion coefficients, α , are a factor of four lower than experimental results.

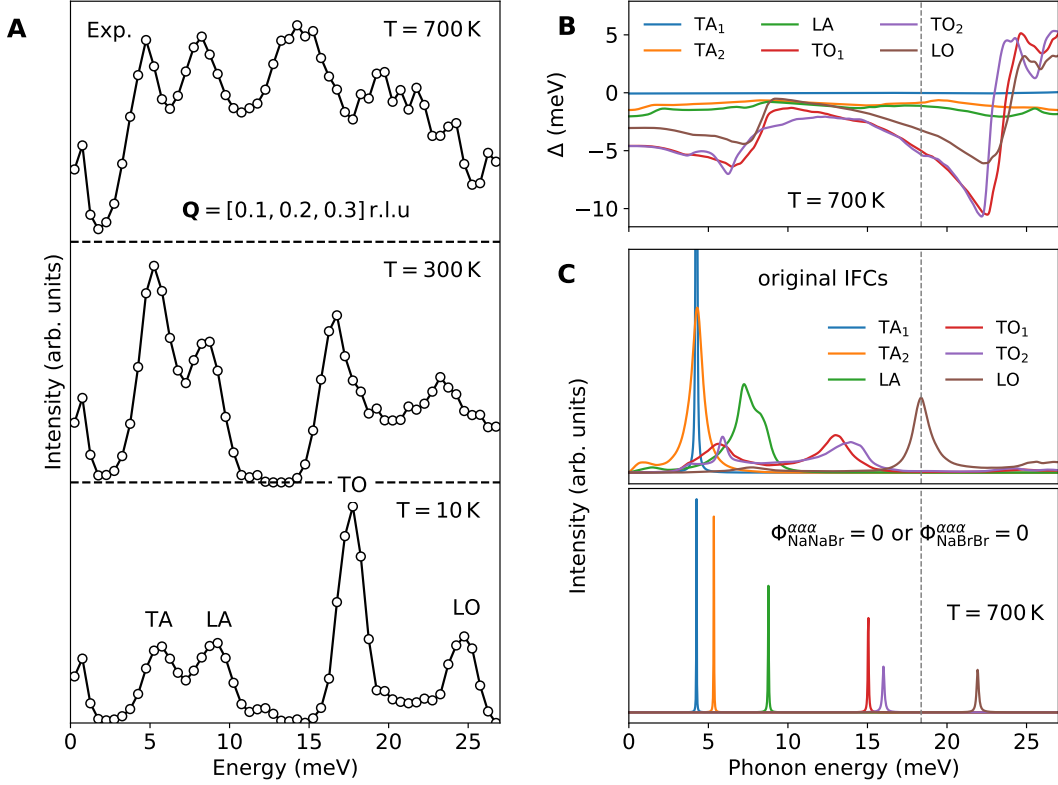


FIG. 4. **Measured and calculated phonon lineshapes at $\mathbf{Q} = [0.1, 0.2, 0.3]$ r.l.u. and the real part of the phonon self-energy.** **a**, The 1D cut of $S(\mathbf{Q}, \varepsilon)$ at a constant $\mathbf{Q} = [0.1, 0.2, 0.3]$ r.l.u. (reciprocal lattice units), showing the temperature dependence of phonon lineshapes in NaBr. At this \mathbf{Q} -point, the LO phonon peak has an energy decrease with temperature of $3 \sim 4$ meV. This can be attributed to the real component of the phonon self-energy as shown in **(b)**. The intensity data were scaled and offset for clarity. **c**, By nulling the third-order force constants, $\Phi_{\text{NaNaBr}}^{\alpha\alpha\alpha}$ or $\Phi_{\text{NaBrBr}}^{\alpha\alpha\alpha}$, associated with the nearest-neighbor degenerate triplets, where $\alpha = (x, y, z)$ represents the direction along the Na-Br bond, the lineshapes at this \mathbf{Q} -point become narrow Lorentzian peaks at 700 K and the energy decrease of the LO mode vanishes.

C. Anharmonic calculations: sTDEP method

With harmonic forces, the instantaneous position (\mathbf{u}_i) and velocity ($\dot{\mathbf{u}}_i$) of the i th atom are the sums of contributions from $3N$ normal modes

$$\mathbf{u}_i = \sum_{s=1}^{3N} \boldsymbol{\epsilon}_{is} A_{is} \sin(\omega_s t + \delta_s), \quad (45)$$

$$\dot{\mathbf{u}}_i = \sum_{s=1}^{3N} \boldsymbol{\epsilon}_{is} A_{is} \omega_s \cos(\omega_s t + \delta_s), \quad (46)$$

where A_s is the normal mode amplitude, δ_s is the phase shift, ω_s and $\boldsymbol{\epsilon}_s$ are eigenvalue and eigenvector corresponding to mode s .

To obtain a set of positions and velocities that correspond to a canonical ensemble, we choose the A_s and δ_s so they are normally distributed around their mean value. Each mode s should contribute, on average, $k_B T/2$ to the internal energy. Then

$$\langle A_{is} \rangle = \sqrt{\frac{\hbar(2n_s + 1)}{2m_i \omega_s}} \approx \frac{1}{\omega_s} \sqrt{\frac{k_B T}{m_i}}, \quad (47)$$

where the approximate result is in the classical limit, $\hbar\omega \ll k_B T$. The appropriate distribution of atomic positions

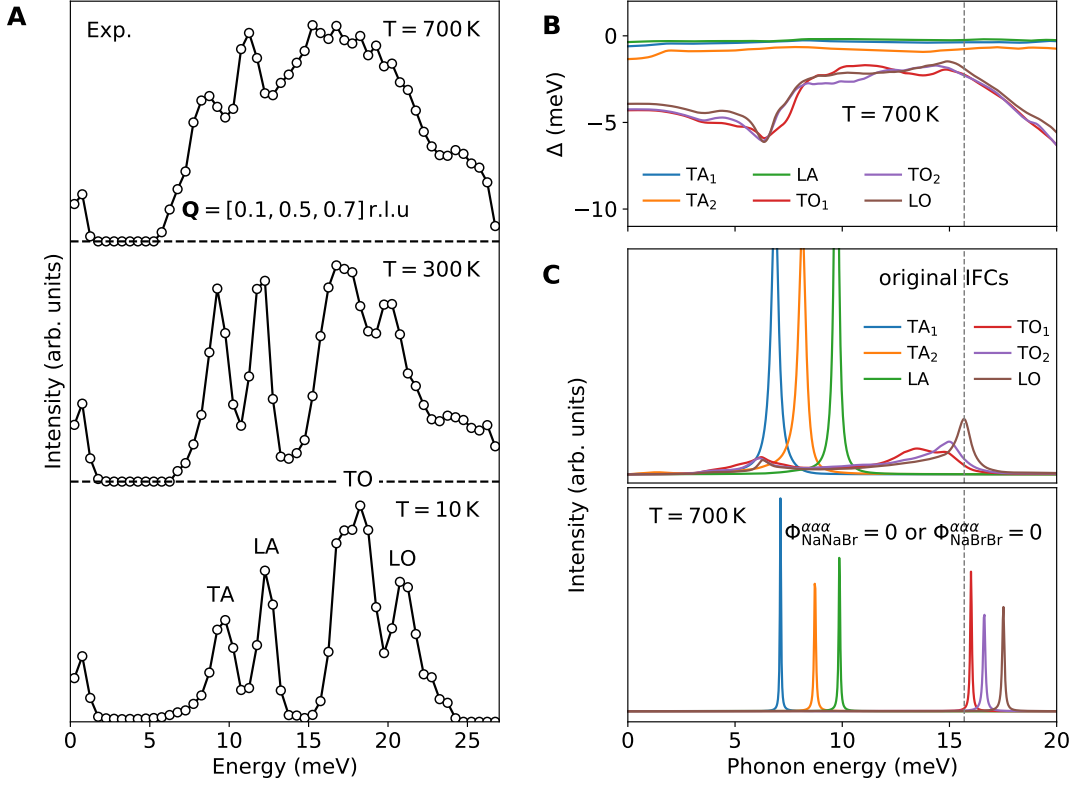


FIG. 5. Measured and calculated phonon lineshapes at $\mathbf{Q} = [0.1, 0.5, 0.7]$ r.l.u. and the real part of the phonon self-energy. The panels are the same quantities in the previous figure, but for $\mathbf{Q} = [0.1, 0.5, 0.7]$ r.l.u. It is seen again that the LO phonon mode shifts to a lower energy at 700 K, mainly due to the cubic interactions.

and velocities are

$$\mathbf{u}_i = \sum_{s=1}^{3N} \epsilon_{is} \langle A_{is} \rangle \sqrt{-2 \ln \xi_1} \sin 2\pi \xi_2, \quad (48)$$

$$\dot{\mathbf{u}}_i = \sum_{s=1}^{3N} \omega_s \epsilon_{is} \langle A_{is} \rangle \sqrt{-2 \ln \xi_1} \cos 2\pi \xi_2, \quad (49)$$

where $\xi_n (n = 1, 2)$ represent a uniform distribution of random numbers between (0, 1), which are transformed to a normal distribution using the standard Box-Muller transform [23, 24].

In practice, we performed first-principles calculations on a temperature-volume grid covering five temperatures and five volumes. We chose the five temperatures as $T = \{10, 300, 450, 600, 700\}$ K and the five volumes linearly spaced within $\pm 5\%$ around the equilibrium volumes. We iterated for 3 to 5 times until the force constants were converged.

Using results from many-body theory, the phonon frequencies were obtained from the dynamical matrix for the constants $\{\Phi_{ij}\}$, and then corrected by the real (Δ) and imaginary (Γ) parts of the phonon self-energy. The imaginary part of the phonon self-energy was calculated with the third-order force constants,

$$\begin{aligned} \Gamma_\lambda(\Omega) = & \frac{\hbar\pi}{16} \sum_{\lambda'\lambda''} |\Phi_{\lambda\lambda'\lambda''}|^2 \{ (n_{\lambda'} + n_{\lambda''} + 1) \\ & \times \delta(\Omega - \omega_{\lambda'} - \omega_{\lambda''}) + (n_{\lambda'} - n_{\lambda''}) \\ & \times [\delta(\Omega - \omega_{\lambda'} + \omega_{\lambda''}) - \delta(\Omega + \omega_{\lambda'} - \omega_{\lambda''})] \}, \end{aligned} \quad (50)$$

where $\Omega (= E/\hbar)$ is the probing energy. The real part was obtained by a Kramers-Kronig transformation

$$\Delta(\Omega) = \mathcal{P} \int \frac{1}{\pi} \frac{\Gamma(\omega)}{\omega - \Omega} d\omega. \quad (51)$$

Equation 50 is a sum over all possible three-phonon interactions, where $\Phi_{\lambda\lambda'\lambda''}$ is the three-phonon matrix element obtained from the cubic force constants Φ_{ijk} by Fourier transformation, n is the Bose-Einstein thermal occupation factor giving the number of phonons in each mode, and the delta functions conserve energy and momentum.

IV. PHONONS AWAY FROM HIGH SYMMETRY LINES

The anharmonicity and its origin with first-neighbor Na-Br bonds are not only true for phonons along the high-symmetry lines, but for the whole Brillouin zone. Figures 4 and 5 (similar to Fig. 3 in the manuscript) show lineshapes from experiment and computation at two arbitrary points in the Brillouin zone, along with the calculated real part of the phonon self-energy. The thermal softening of the LO phonon modes at 700 K is seen over the Brillouin zone. The real part of the phonon self-energy, arising from cubic anharmonicity to second order, is the main cause of these thermal shifts and broadenings.

-
- [1] P. B. Allen, Quasi-harmonic theory of thermal expansion, [arXiv preprint arXiv:1906.07103](#) (2019).
 - [2] D. C. Wallace, *Statistical Physics of Crystals and Liquids* (World Scientific, Singapore, 2002) p. 193.
 - [3] R. A. Cowley, Zero sound, first sound and second sound of solids, *Proc. Phys. Soc.* **90**, 1127 (1967).
 - [4] J. A. Reissland, *The Physics of Phonons* (Wiley-Interscience, London, UK, 1973) Chap. 7.4.
 - [5] O. L. Anderson, Derivation of Wachtman's equation for the temperature dependence of elastic moduli of oxide compounds, *Phys. Rev.* **144**, 553 (1966).
 - [6] A. S. M. Rao, K. Narender, K. G. K. Rao, and N. G. Krishna, Thermophysical properties of NaCl, NaBr and NaF by γ -ray attenuation technique, *J. Mod. Phys.* **4**, 208 (2013).
 - [7] Y. Sato-Sorensen, Phase transitions and equations of state for the sodium halides: NaF, NaCl, NaBr, and NaI, *J. Geophys. Res. Solid Earth* **88**, 3543 (1983).
 - [8] V. F. Sears, Incoherent neutron scattering for large momentum transfer. ii. quantum effects and applications, *Phys. Rev. A* **7**, 340 (1973).
 - [9] G. Kresse and J. Hafner, *Ab initio* molecular dynamics for liquid metals, *Phys. Rev. B* **47**, 558 (1993).
 - [10] G. Kresse and J. Hafner, *Ab initio* molecular-dynamics simulation of the liquid-metal-amorphous-semiconductor transition in germanium, *Phys. Rev. B* **49**, 14251 (1994).
 - [11] G. Kresse and J. Furthmüller, Efficiency of ab-initio total energy calculations for metals and semiconductors using a plane-wave basis set, *Comput. Mater. Sci.* **6**, 15 (1996).
 - [12] G. Kresse and J. Furthmüller, Efficient iterative schemes for *ab initio* total-energy calculations using a plane-wave basis set, *Phys. Rev. B* **54**, 11169 (1996).
 - [13] G. Kresse and D. Joubert, From ultrasoft pseudopotentials to the projector augmented-wave method, *Phys. Rev. B* **59**, 1758 (1999).
 - [14] J. P. Perdew, K. Burke, and M. Ernzerhof, Generalized gradient approximation made simple, *Phys. Rev. Lett.* **77**, 3865 (1996).
 - [15] A. Togo and I. Tanaka, First principles phonon calculations in materials science, *Scr. Mater.* **108**, 1 (2015).
 - [16] O. Hellman, I. A. Abrikosov, and S. I. Simak, Lattice dynamics of anharmonic solids from first principles, *Phys. Rev. B* **84**, 180301 (2011).
 - [17] O. Hellman, P. Steneteg, I. A. Abrikosov, and S. I. Simak, Temperature dependent effective potential method for accurate free energy calculations of solids, *Phys. Rev. B* **87**, 104111 (2013).
 - [18] O. Hellman and I. A. Abrikosov, Temperature-dependent effective third-order interatomic force constants from first principles, *Phys. Rev. B* **88**, 144301 (2013).
 - [19] M. Gajdoš, K. Hummer, G. Kresse, J. Furthmüller, and F. Bechstedt, Linear optical properties in the projector-augmented wave methodology, *Phys. Rev. B* **73**, 045112 (2006).
 - [20] X. Gonze and C. Lee, Dynamical matrices, born effective charges, dielectric permittivity tensors, and interatomic force constants from density-functional perturbation theory, *Phys. Rev. B* **55**, 10355 (1997).
 - [21] G. K. White, J. G. Collins, and K. A. G. Mendelsohn, The thermal expansion of alkali halides at low temperatures - II. Sodium, rubidium and caesium halides, *Proc. R. Soc. Lond. A* **333**, 237 (1973).
 - [22] J. E. Rapp and H. D. Merchant, Thermal expansion of alkali halides from 70 to 570 K, *J. Appl. Phys.* **44**, 3919 (1973).
 - [23] D. C. Wallace, *Thermodynamics of crystals* (Wiley, New York, US, 1972).
 - [24] N. Shulumba, O. Hellman, and A. J. Minnich, Intrinsic localized mode and low thermal conductivity of PbSe, *Phys. Rev. B* **95**, 014302 (2017).